

## AEROSOL RETROACTION ON THE AIR IN A TWO-DIMENSIONAL BRANCH \*

L. BOUDIN<sup>1,2</sup>, A. DEVYS<sup>3,4</sup>, C. GRANDMONT<sup>2</sup>, B. GREC<sup>5</sup> AND D. YAKOUBI<sup>2</sup>

**Abstract.** In this work, we investigate two different aspects of an aerosol behaviour in the human airways. After a brief presentation of the model, we first study the impingement of aerosol particles with respect to their Stokes number and obtain again some well-known results. Then we consider the effect of an aerosol on the airflow and obtain a range of particles size where the aerosol action on the air cannot be neglected.

### 1. INTRODUCTION

The aerosols are often used as a medical treatment of respiratory/lung diseases. The aerosol therapy consists in delivering medication in a mist form the patient must breathe in. There are lots of works about the aerosol behaviour and deposition in the human airways, most of them dedicated to the upper part of the airways. For example, one can check [2,7,8,11,16] and the references therein. They often aim to compare experimental data and numerical results. The human respiratory tract can be classically described by a branched structure, see for instance [3,12,13,17]. It is relevant to focus on one branch to investigate some properties of the aerosol.

The present work has two main goals. The first one is to recover some results [1,18] about particle deposition with respect to the associated Stokes number in a two-dimensional one-generation bifurcation mimicking the trachea and the first bronchi. The second one is to estimate the influence of the aerosol on the airflow in the same geometry of the human airways. Indeed, the airflow has an indisputable effect on the aerosol through a drag (or friction) force. Conversely, it is commonly admitted in the literature that the so-called retroaction of the aerosol on the air can be neglected. This work is hence an attempt to quantify this statement, noting that, in [11], for instance, the retroaction is taken into account in the model and the computations.

The airflow can be described by the incompressible Navier-Stokes equations down to the seventh generation of the respiratory tract. The medical aerosols are constituted of very numerous particles, so that direct numerical simulations happen to be too expensive. Relying on the kinetic theory of rarefied gases and its statistical mechanics viewpoint seems to be a good solution to model an aerosol.

---

\* This work was partially funded by the ANR-08-JCJC-013-01 project headed by C. Grandmont.

<sup>1</sup> UPMC Paris 06, Lab. J.-L. Lions, 175 rue du Chevaleret, BC 187, F-75013 Paris, France;  
e-mail: laurent.boudin@upmc.fr

<sup>2</sup> INRIA Paris-Rocquencourt, REO Project team, BP 105, F-78153 Le Chesnay Cedex, France;  
e-mail: celine.grandmont@inria.fr & driss.yakoubi@inria.fr

<sup>3</sup> UST Lille, Lab. P. Painlevé, Cité Scientifique, F-59655 Villeneuve d'Ascq Cedex, France;  
e-mail: anne.devys@math.univ-lille1.fr

<sup>4</sup> INRIA Lille Nord Europe, SIMPAF Project team, B.P. 70478, F-59658 Villeneuve d'Ascq Cedex, France;

<sup>5</sup> Université Claude Bernard Lyon 1, Institut C. Jordan, F-69622 Villeurbanne Cedex, France;  
e-mail: grec@math.univ-lyon1.fr

## 2. AEROSOL MODELLING AND SIMULATION

### 2.1. Model

The situations we deal with in this work are only two-dimensional. The airflow can be described by its velocity field  $u(t, x) \in \mathbb{R}^2$  and the pressure  $p(t, x) \in \mathbb{R}$ , where  $t \geq 0$  is the time and  $x \in \mathbb{R}^2$  is the space location. Since the air is assumed to be incompressible, the air density remains constant, denoted by  $\varrho_{\text{air}}$ . Inside the human body, at temperature 310K, one can take  $\varrho_{\text{air}} = 1.11 \text{ kg.m}^{-3}$ . Let us also denote  $\nu$  the air kinematic viscosity and  $\mu = \varrho_{\text{air}} \nu$  the dynamic one. A standard value of  $\mu$  is  $1.88 \times 10^{-5} \text{ kg.m}^{-1}.\text{s}^{-1}$ . The previous values can be found, for instance, in [1].

As already stated, a kinetic equation seems to be a good mean to model the behaviour of an aerosol [4,11]. The aerosol itself is described by a probability density function (PDF), which we denote  $f$ . The PDF depends not only on  $t$  and  $x$ , but also on velocity  $v \in \mathbb{R}^2$ . In fact,  $f$  can also depend on the particle radius  $r$  (we here assume that the particles remain spherical). Let us emphasize that we shall not take into account any phenomenon modifying the aerosol radius distribution (no collision, no abrasion, *etc.*). This means that the initial radius distribution is conserved. Therefore, the radius will not appear as a variable in the equations, but only as a parameter. The dependence of  $f$  on  $r$  allows to send particles with various radii in the computational domain  $\Omega$ .

Dependence on other physical quantities, like temperature, is not discussed here, but one can easily admit that, for instance, the temperature variation has a negligible influence on the phenomena in the airways, in standard conditions. In the following, we assume that the aerosol is also an incompressible fluid very similar to the water, so that its volume mass  $\varrho_{\text{aero}}$  can be chosen as  $\varrho_{\text{aero}} = 1000 \text{ kg.m}^{-3}$ . Then, for each particle with radius  $r$ , we can use its mass  $m = 4/3 \pi r^3 \varrho_{\text{aero}}$ .

The quantity  $f(t, x, v, r) dr dv dx$  is then the number of particles at time  $t$  inside the elementary volume centered at  $(x, v, r)$  in the phase space. Eventually, here is the full system satisfied by  $f$ ,  $u$  and  $p$ :

$$\partial_t u + \nabla_x \cdot (u \otimes u) - \nu \Delta_{xx} u + \frac{\nabla_x p}{\varrho_{\text{air}}} = \frac{\mathcal{F}_{\text{aero}}}{\varrho_{\text{air}}}, \quad (1)$$

$$\nabla_x \cdot u = 0, \quad (2)$$

$$\partial_t f + \nabla_x \cdot (vf) + \nabla_v \cdot (af) = 0, \quad (3)$$

where  $a$  is the particle acceleration, mainly due here to the Stokes force exerted on the aerosol by the fluid, and is given by

$$a(t, x, v, r) = \frac{6\pi\mu r}{m(r)} (u(t, x) - v), \quad (4)$$

and  $\mathcal{F}_{\text{aero}}$  is the force exerted by the aerosol on the air, that is

$$\mathcal{F}_{\text{aero}}(t, x) = - \iint_{\mathbb{R}^2 \times \mathbb{R}_+} f(t, x, v, r) m(r) a(t, x, v, r) dv dr = 6\pi\mu \iint_{\mathbb{R}^2 \times \mathbb{R}_+} r f(t, x, v, r) (v - u(t, x)) dv dr. \quad (5)$$

This system was mathematically investigated in [5] in a periodic in space framework, and without any dependence on  $r$ .

The boundary  $\Gamma = \partial\Omega$  of the computational domains we shall consider can be divided into three areas, not necessarily connate: the inlet  $\Gamma_{\text{in}}$ , the outlet(s)  $\Gamma_{\text{out}}$  and the wall  $\Gamma_{\text{wall}}$ . Figure 1 shows the typical domain on which we perform computations: a branch.

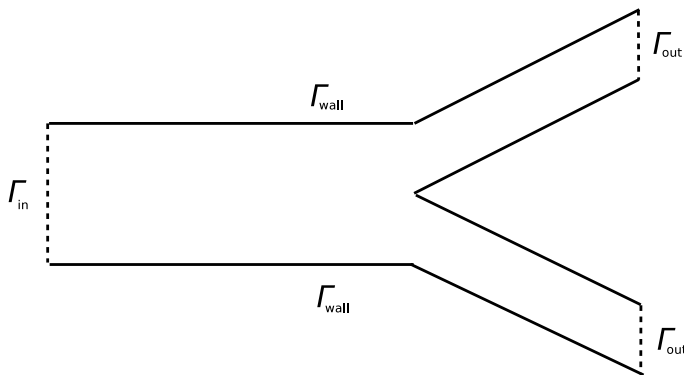


FIGURE 1. Standard branch with boundaries

Equations (1)–(5) must then be supplemented with boundary conditions:

$$u(t, x) = \tilde{u}(t, x) \quad \text{if } x \in \Gamma_{\text{in}}, \quad (6)$$

$$u(t, x) = 0 \quad \text{if } x \in \Gamma_{\text{wall}}, \quad (7)$$

$$v \frac{\partial u}{\partial n}(t, x) - p(t, x) n(x) = 0 \quad \text{if } x \in \Gamma_{\text{out}}, \quad (8)$$

$$f(t, x, v, r) = \tilde{f}(t, x, v, r) \quad \text{if } x \in \Gamma_{\text{in}}, \quad (9)$$

$$f(t, x, v, r) = 0 \quad \text{if } x \in \Gamma_{\text{wall}} \text{ and } v \cdot n(x) < 0, \quad (10)$$

where  $\tilde{u}$  (resp.  $\tilde{f}$ ) is the profile of the incoming velocity (resp. the incoming particle distribution) in  $\Omega$ . Condition 10 has been discussed in [6],  $n(x)$  being the outgoing normal vector to  $\Gamma$  in  $x$ .

## 2.2. Numerical solving

The airflow is solved by a standard  $P^1 - P^2$  finite element computation, and the aerosol by a particle method. We do not give any detail on the fluid computation, since (1)–(2), (6)–(7) are solved thanks to a Navier-Stokes routine using the `FreeFem++` software [14]. For the particle method, we have to distinguish the physical particles from the numerical ones. The total number of numerical particles  $N$  is almost always much smaller than the number of real physical particles  $N_P$ . The PDF  $f$  can discretized in the following way

$$f(t, x, v, r) = \sum_{p=1}^N \omega_p(t) \delta_{x_p(t)}(x) \delta_{v_p(t)}(v) \delta_{r_p(t)}(r),$$

where  $t \mapsto (x_p(t), v_p(t), r_p(t))$  is the trajectory of the numerical particle  $p$  in the phase space, and  $\omega_p(t)$  its representativity at time  $t$ . A numerical particle  $p$  gives an average behaviour of a set of physical particles. The average value of  $\omega_p$  is approximately of the order  $N_P/N$ . Note that our numerical code is inspired from an engineering project performed under B. Maury's supervision [9].

In the following, we always assume that the incoming velocity boundary condition on  $\Gamma_{\text{in}}$  has a Poiseuille parabolic profile, with maximum value equal to 1. We can check on Figure 2 that the air velocity field has the numerically awaited behaviour (in particular, it remains between 0 and 1).

## 3. STUDY OF THE AEROSOL FLOW WITH RESPECT TO THE STOKES NUMBER

The Stokes number  $St$  is classically used to describe the behavior of particles evolving in a fluid flow with an obstacle. Its primary definition, when the particle is suspended in an ambient fluid, depends on the fluid

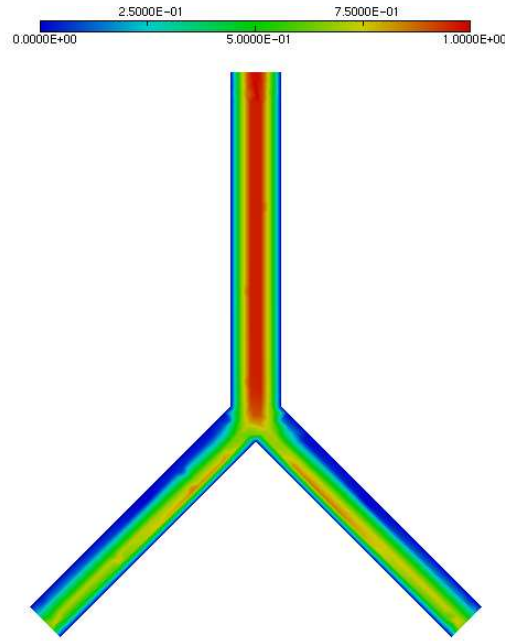


FIGURE 2. Air velocity field

velocity, the characteristic size of the obstacle and other quantities of the fluid and the aerosol. If  $St \gg 1$ , the particle hits the obstacle, and if  $St \ll 1$ , the particle still follows the fluid streamlines. In our context, the obstacle is the wall itself, and the particles have their own velocities. The Stokes number can then be given [1] (see also [18]) by

$$St = \frac{4 \rho_{\text{aero}} r^2 |v|}{9 \mu D}, \quad (11)$$

where  $D$  is the local diameter of the respiratory tree.

Since we study the branch case, we can choose  $D$  as the diameter of the lower part of the tree, that is, in the 2D Weibel model (see [17], for instance),  $D_1 = 0.0141$  m. This two-dimensional model has the advantage to conserve the resistance of the three-dimensional airways, but loses other significant quantities, such as the air Reynolds number. Since  $v$  varies for each particle and during the computation, but still satisfies  $|v| \leq 1$ , we compute the Stokes number with  $|v| = 1$ , that ensures to obtain the smallest possible value of  $St$ .

We send inside the domain 50 particles sharing the same Stokes number at each computational experiment. For the highest values of  $St$ , we recover that almost every particle hits the angle of the branch (see Fig. 3 obtained thanks to the visualization software `medit` [10]).

Figure 4 shows the numerical graph of the number of outgoing particles with respect to the Stokes number. It is very clear that there is an optimal value near  $St = 10^{-4.5} = 3.17 \times 10^{-5}$ , which corresponds to a radius approximately equal to 100 nm. We qualitatively recover the experimental values obtained in [15]. Note that the particles still deposit even for very small  $St$  because  $St$  is a mean value, and the real values of  $St$  for the depositing particles are in fact higher.

Most aerosol inhalers generate a lognormal distribution in the variable  $r$ . It would be easy to draw the following conclusion. Since we want to reach an area located in the lower airways, we have to choose the ingoing distribution centered at the optimal radius obtained with the corresponding optimal Stokes number. Of course, it is not that simple: the fact that a certain amount of aerosol actually goes out from the upper airways (say,

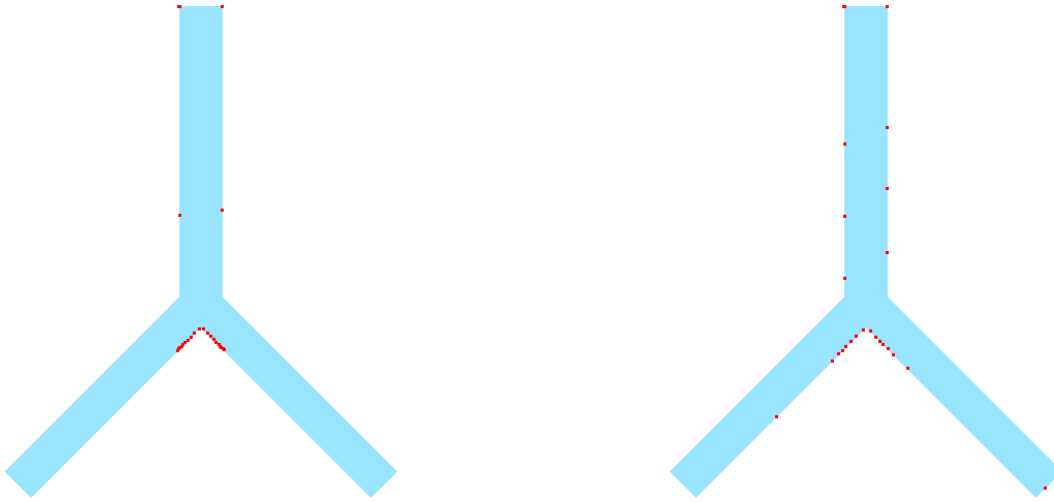


FIGURE 3. Aerosol deposition areas for (a)  $St = 26.2$ , and (b)  $St = 9.42$

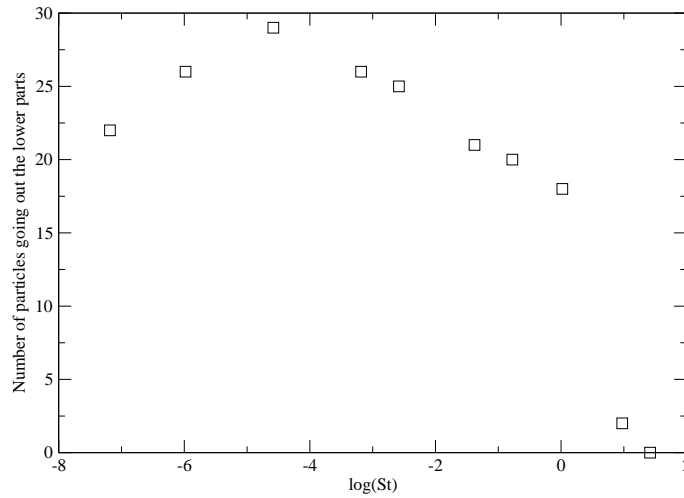


FIGURE 4. Counting outgoing particles with respect to  $\log_{10}(St)$

after the seventh generation) does not imply that it will eventually reach the lower parts (after the seventeenth generation). Other studies have to be led, since, among other reasons, between the seventh and the seventeenth generations, the airflow and aerosol models used here may not hold.

#### 4. RETROACTION OF THE AEROSOL ON THE FLUID

The presence of the term  $\mathcal{F}_{aero}$  in (1) is the second topic of this work. It does not concern the aerosol itself, but its influence on the airflow. In fact, it really matters to understand and foresee whether this retroaction force

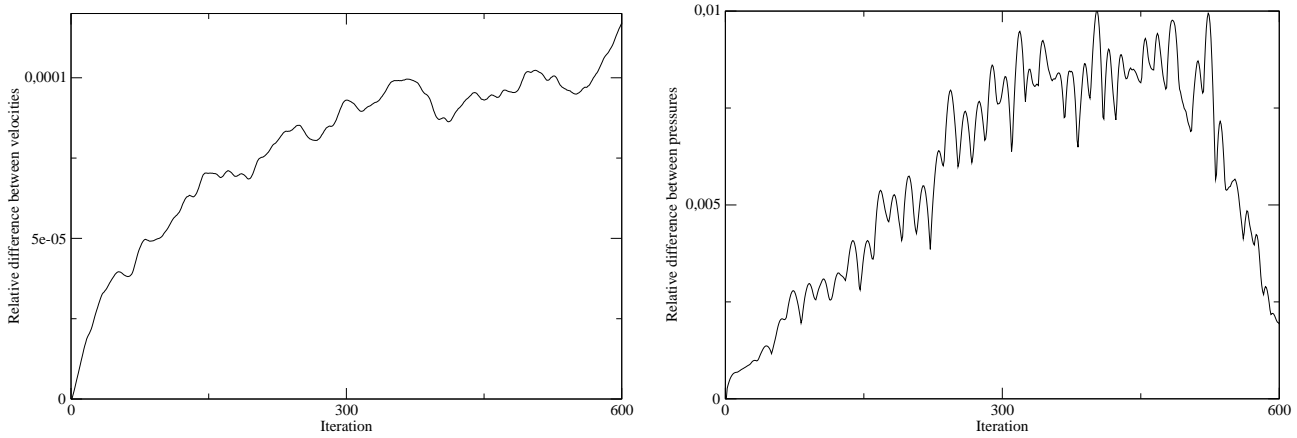


FIGURE 5. Plot of (a)  $\varepsilon_u$  and (b)  $\varepsilon_p$ , for  $r = 100 \mu\text{m}$  and  $\omega_p = 10^4$

of the aerosol on the fluid is to be taken into account, depending on various parameters, such as the particle radius or the total number of particles.

As in Section 3, we study the case of a branch representing the first branch of the airways (its upper diameter is  $D_0 = 0.018 \text{ m}$ ). The particles are initially uniformly distributed on the boundary  $\Gamma_{\text{in}}$ , and injected in  $\Omega$  at time  $t = 0$  with a vertical velocity constant equal to  $v = 2$ . In each case, 10 000 particles are injected, but their representativity  $\omega_p$  may vary with regard to each test. The time step is fixed equal to  $\Delta t = 10^{-4} \text{ s}$ . The computations are relevant as long as there remain some particles in the domain.

We performed computations in four situations. The tests are carried out for two different radii of the particles ( $r = 100 \mu\text{m}$  and  $r = 1 \mu\text{m}$ ) and two different particle representativities ( $\omega_p = 10^4$  or  $\omega_p = 10^2$  particles) independent of  $t$ . Note that such values are not necessarily physically relevant for the respiratory aerosols, but they are used for numerical validations.

In each case, we compute the velocity field  $u$  (resp.  $u_{\text{ref}}$ ) and the pressure  $p$  (resp.  $p_{\text{ref}}$ ) with (resp. without) the retroaction force  $\mathcal{F}_{\text{aero}}$ . We compute a relative difference for the velocity and the pressure at each time step:

$$\varepsilon_u = \frac{\|u - u_{\text{ref}}\|_{L^2}}{\|u_{\text{ref}}\|_{L^2}}, \quad \varepsilon_p = \frac{\|p - p_{\text{ref}}\|_{L^2}}{\|p_{\text{ref}}\|_{L^2}}.$$

The choice of the  $L^2$  norm is convenient to be computed. It is also interesting to compute a relative  $L^\infty$  difference between the two cases. First computational observations indicate that the  $L^\infty$  norm remains about ten times bigger than the  $L^2$  one, and thus that the retroaction does not generate big variations at some points in the domain. Therefore, it is relevant to determine whether the retroaction is negligible by computing with the  $L^2$  norm.

#### 4.1. Large representativity of big particles

We first choose  $r = 100 \mu\text{m}$  and  $\omega_p = 10^4$ . In this case, we see on Figure 5 that the aerosol retroaction has a rather significant effect on the velocity field, and a really significant one on the pressure.

The computation lasts for approximately 600 timesteps, because the aerosol is fully deposited around this time. In order to follow the evolution of the particles with respect to time, we represent the retroaction force field at  $t = 0$ ,  $t = 200 \Delta t$ ,  $t = 400 \Delta t$ ,  $t = 600 \Delta t$  on Figure 6.

We observe that at time  $t = 600 \Delta t$ , the particles are deposited on the angle of the branch, where the force is almost equal to 0. Note that there is a residual component of  $\mathcal{F}_{\text{aero}}$  in the top of the branch, because there remain some particles with very low velocities near the wall.

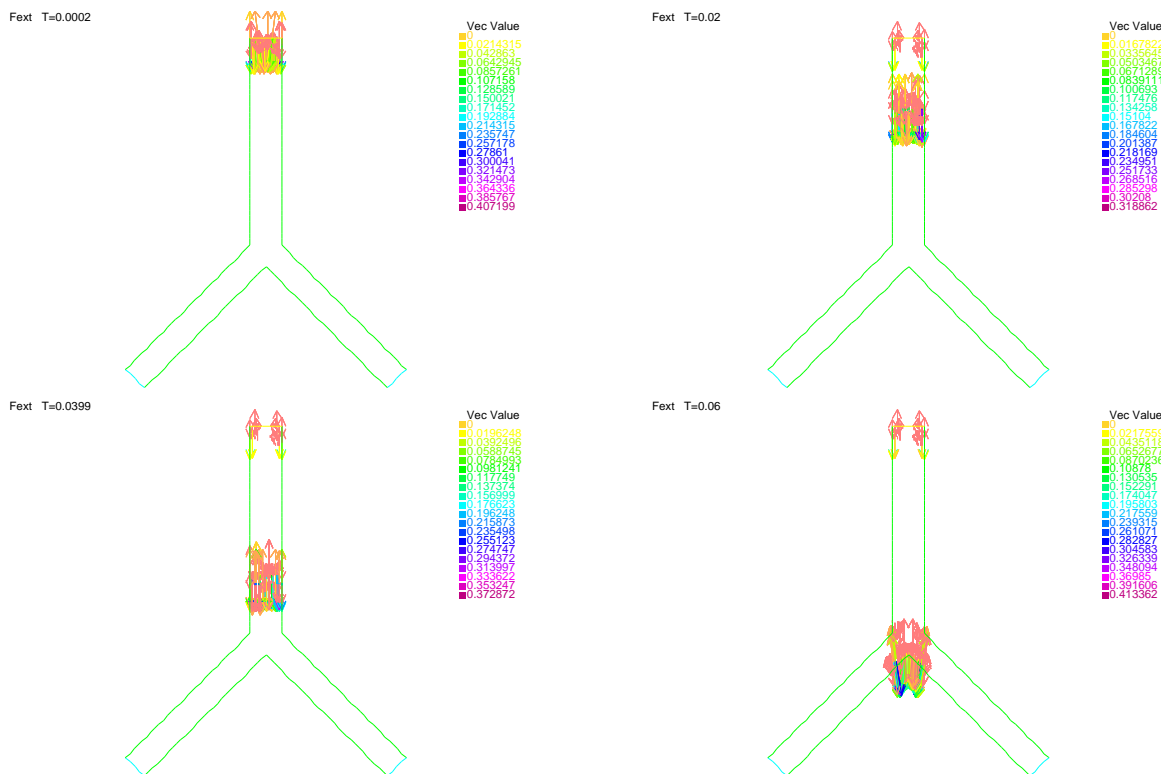


FIGURE 6. Retroaction force  $\mathcal{F}_{aero}$  at (a)  $t = 0$ , (b)  $t = 200 \Delta t$ , (c)  $t = 400 \Delta t$  and (d)  $t = 600 \Delta t$

Figure 7 shows the pressure gradient  $\nabla_x p$  for the same times as the retroaction force. We observe that the pressure force seems to be more significant than the retroaction one. Therefore, in (1), the fluid velocity is mostly determined by the pressure gradient. Besides, we can compute the relative weight of the retroaction:

$$\varepsilon_{\mathcal{F}} = \frac{\|\mathcal{F}_{aero}\|_{\infty}}{\|\nabla p\|_{\infty}}.$$

With the values of Figure 6 and 7, we obtain that  $\varepsilon_{\mathcal{F}} \simeq 10^{-3}$ . Actually, this order of magnitude corresponds to the values obtained for the differences between velocities in the  $L^{\infty}$  norm, and thus explains these values.

#### 4.2. Small representativity of big particles

In this second situation, we pick  $r = 100 \mu\text{m}$  and  $\omega_p = 10^2$ . Figure 8 shows that the velocity relative difference is at most  $1.2 \times 10^{-6}$ , which seems quite negligible in most computations. Nevertheless, the pressure relative difference almost reaches  $10^{-4}$ , with a notable peak at the beginning of the computation. In fact, we can already find such a peak in Figure 5, but it is not really clear, because the computation has then to be stopped after the particle deposited. An explanation of this peak would be that the incoming particles generate a shockwave which mainly appears on the pressure.

#### 4.3. Large representativity of small particles

We here choose  $r = 1 \mu\text{m}$  and  $\omega_p = 10^4$ . The behaviors of both  $\varepsilon_u$  and  $\varepsilon_p$  in Figure 9 are quite similar to the ones in Figure 8. The pressure peak is lower than the one of Figure 8, but of the same order, whereas the velocity difference is ten times smaller. In any case, the retroaction seems to be negligible.

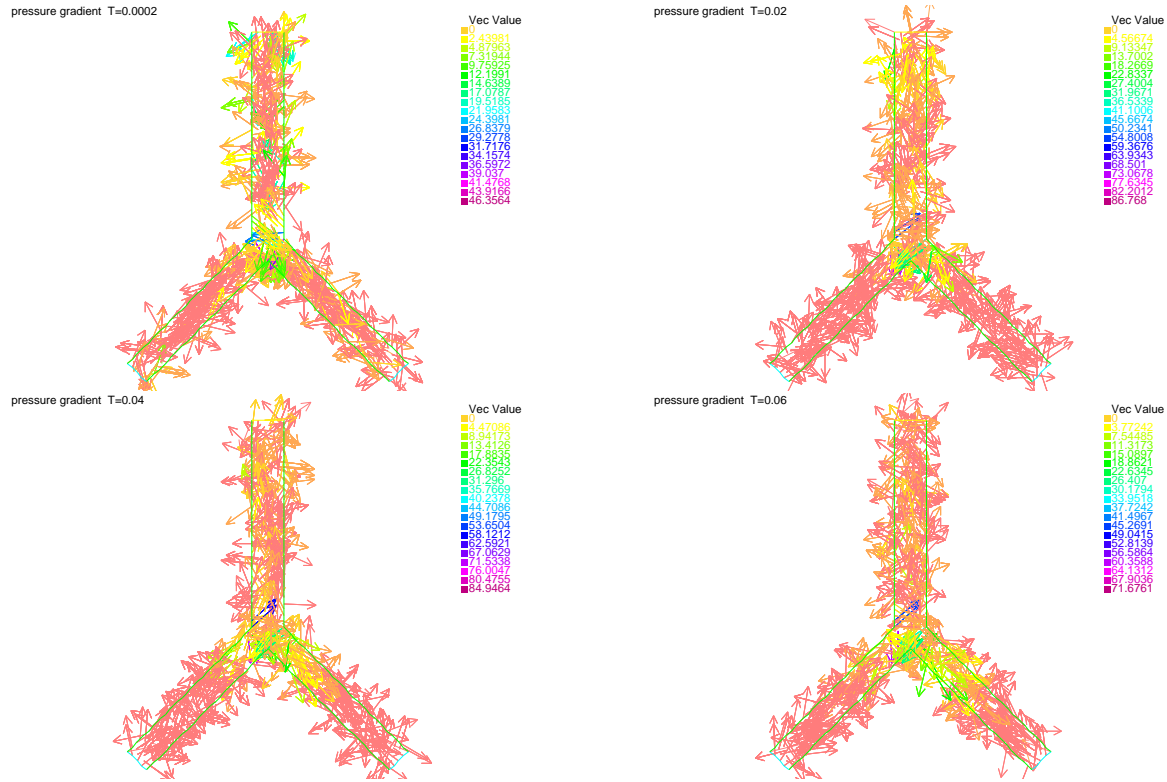


FIGURE 7. Pressure gradient  $\nabla_x p$  at (a)  $t = 0$ , (b)  $t = 200 \Delta t$ , (c)  $t = 400 \Delta t$  and (d)  $t = 600 \Delta t$

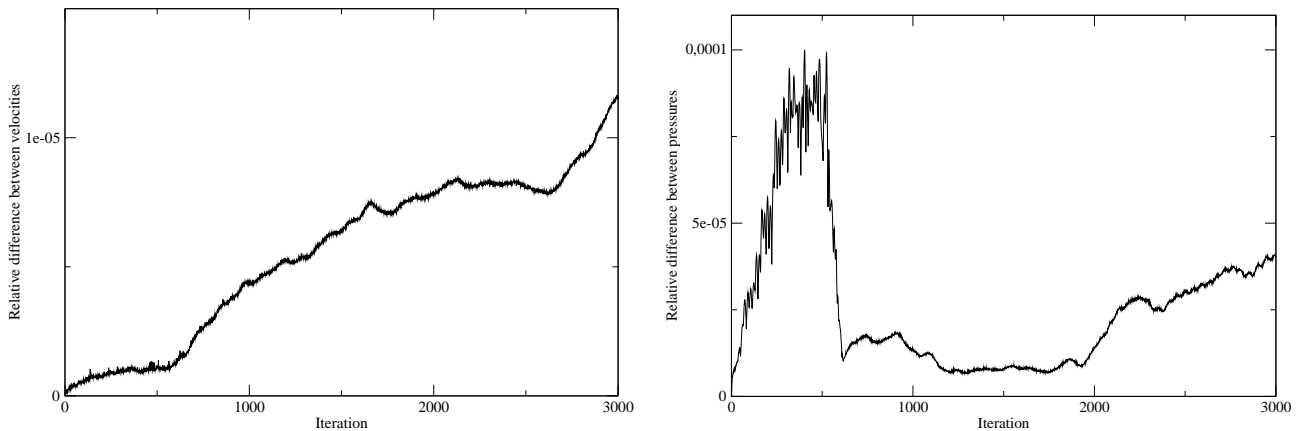


FIGURE 8. Plot of (a)  $\varepsilon_u$  and (b)  $\varepsilon_p$ , for  $r = 100 \mu\text{m}$  and  $\omega_p = 10^2$

#### 4.4. Small representativity of small particles

Eventually, we pick  $r = 1 \mu\text{m}$  and  $\omega_p = 10^2$ . The results corresponding to this case are represented in Figure 10. We recover the fact that if the particle size and the particle number are low, the retroaction of the aerosol has very little effect on the fluid. In fact, the relative difference between the velocity fields is around  $10^{-7}$ , which is much smaller than the other cases.

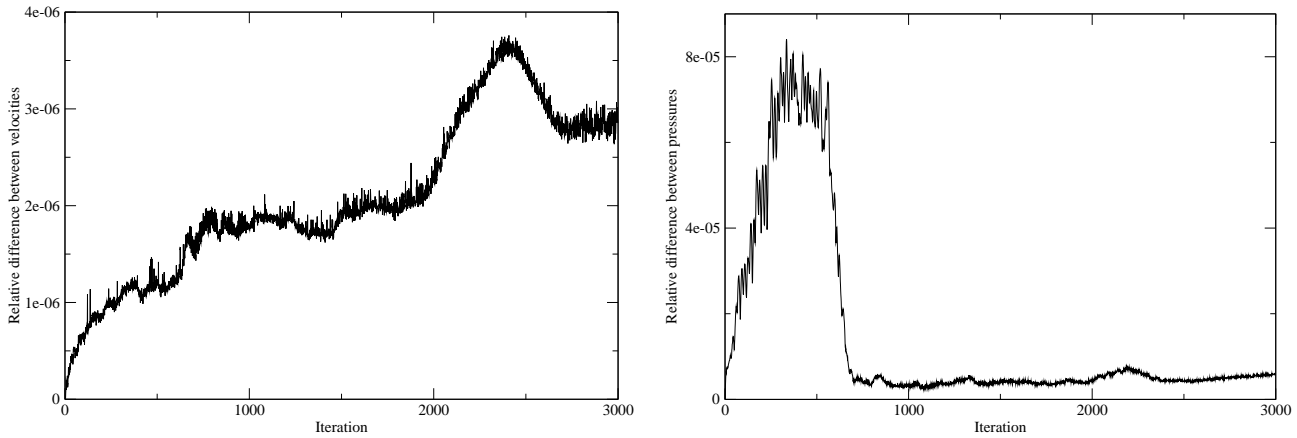


FIGURE 9. Plot of (a)  $\varepsilon_u$  and (b)  $\varepsilon_p$ , for  $r = 1 \mu\text{m}$  and  $\omega_p = 10^4$

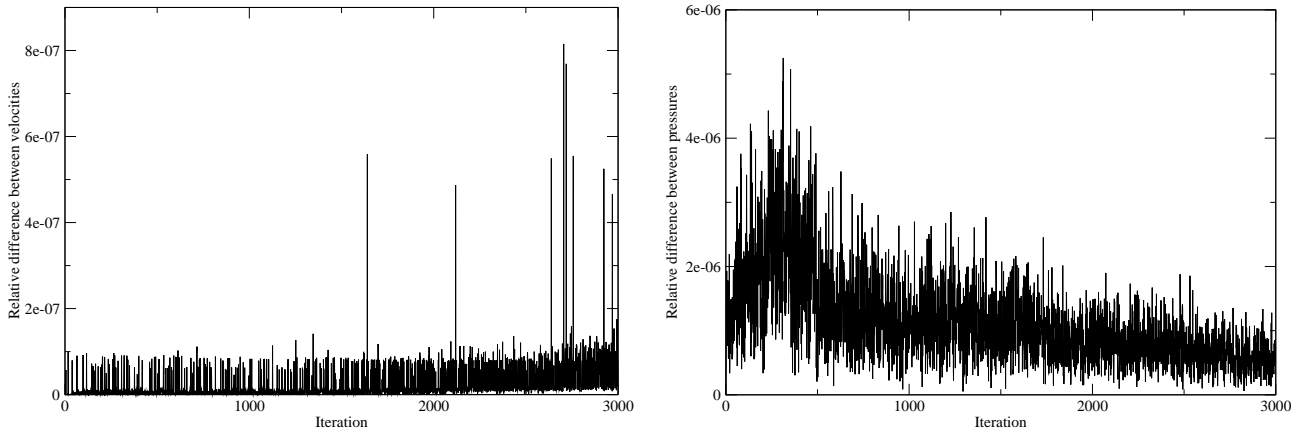


FIGURE 10. Plot of (a)  $\varepsilon_u$  and (b)  $\varepsilon_p$ , for  $r = 1 \mu\text{m}$  and  $\omega_p = 10^2$ .

#### 4.5. Conclusion

Those four tests allow us to state that there is a strong dependence of the retroaction force on the particle radius and the numerical representativity. Both parameters have an influence on the mass of a numerical particle. It is then clear that, even if we send small particles inside the branch, and by extension in the upper airways, the aerosol may have some (weak but not necessarily negligible) influence on the air. Moreover, near the seventh generation, this retroaction may be more significant too.

Eventually, we have to point out again that our conclusions have been obtained in a two-dimensional framework, more precisely with the Weibel model. The difference between two- and three-dimensional models, for example, the fact that the resistance of the tree and the air Reynolds number cannot be simultaneously conserved, imply that the same question about the aerosol retroaction must be tackled in the three-dimensional case.

**Acknowledgement.** The authors want to thank Sébastien Martin and Bertrand Maury for the very helpful scientific discussions which took place during Cemracs 2008, and Frédéric Hecht and Mourad Ismail for their support for the **Freefem++** use for the project.

## REFERENCES

- [1] J.E. Agnew, D. Pavia, and S.W. Clarke. Aerosol particle impaction in the conducting airways. *Phys. Med. Biol.*, 29:767–777, 1984.
- [2] G. M. Allen, B. P. Shortall, T. Gemci, T. E. Corcoran, and N. A. Chigier. Computational simulations of airflow in an in vitro model of the pediatric upper airways. *J. Biomech. Eng.*, 26:604–613, 2004.
- [3] L. Baffico, C. Grandmont, and B. Maury. Multiscale modelling of the respiratory track. HAL, 2008. Submitted, available at <http://hal.inria.fr/inria-00343629/en/>.
- [4] C. Baranger, L. Boudin, P.-E. Jabin, and S. Mancini. A modeling of biospray for the upper airways. *ESAIM Proc.*, 14:41–47, sep 2005.
- [5] L. Boudin, L. Desvillettes, C. Grandmont, and A. Moussa. Global existence of solutions for the coupled Vlasov and Navier-Stokes equations. *Differential Integral Equations*, 2009. Accepted, available at <http://hal.archives-ouvertes.fr/hal-00331895/fr/>.
- [6] L. Boudin and L. Weynans. Spray impingement on a wall in the context of the upper airways. *ESAIM Proc.*, 23:1–9, 2008.
- [7] J. K. Comer, C. Kleinstreuer, and Z. Zhang. Flow structures and particle deposition patterns in double bifurcation airway models. part 1. air flow fields. *J. Fluid Mech.*, 435:25–54, 2001.
- [8] J. K. Comer, C. Kleinstreuer, and Z. Zhang. Flow structures and particle deposition patterns in double bifurcation airway models. part 2. aerosol transport and deposition. *J. Fluid Mech.*, 435:55–80, 2001.
- [9] J. Crest and Q. Dérumeaux. Modélisation du dépôt de particules dans les bronches. Technical report, École Polytechnique, 2007.
- [10] C. Dobrzynski and P. Frey. Medit, scientific visualization software, <http://www.ann.jussieu.fr/~frey/logiciels/medit.html>.
- [11] T. Gemci, T. E. Corcoran, and N. Chigier. A numerical and experimental study of spray dynamics in a simple throat model. *Aerosol Sci. Technol.*, 36:18–38, 2002.
- [12] C. Grandmont, Y. Maday, and B. Maury. A multiscale/multimodel approach of the respiration tree. In *New trends in continuum mechanics*, volume 3 of *Theta Ser. Adv. Math.*, pages 147–157. Theta, Bucharest, 2005.
- [13] C. Grandmont, B. Maury, and A. Soualah. Multiscale modelling of the respiratory track: a theoretical framework. *ESAIM Proc.*, 23:10–29, 2008.
- [14] F. Hecht, A. Le Hyaric, K. Ohtsuka, and O. Pironneau. Freefem++, finite elements software, <http://www.freefem.org/ff++/>.
- [15] J. Löndahl, J. Pagels, E. Swietlicki, J. Zhou, M. Ketzler, A. Massling, and M. Bohgard. A set-up for field studies of respiratory tract deposition of fine and ultrafine particles in humans. *Aerosol Science*, 37:1152–1163, 2006.
- [16] T. R. Sosnowski, A. Moskai, and L. Gradon. Mechanisms of aerosol particle deposition in the oro-pharynx under non steady airflow. *Ann. Occup. Hyg.*, 51:19–25, 2007.
- [17] A. Soualah-Alilah. *Modélisation mathématique et numérique du poumon humain*. PhD thesis, Université Paris-Sud–Orsay, 2007.
- [18] T.F. Vasconcelos, M. Filoche, J.S. Andrade, and B. Sapoval. Iterative trapping of advected particles into a branched structure. In Luciano Pietronero, Vittorio Loreto, and Stefano Zapperi, editors, *Abstract Book of the XXIII IUPAP International Conference on Statistical Physics*. Genova, Italy, 9-13 July 2007.